Electronic band structure trends of perovskite halides: Beyond Pb and Sn to Ge and Si

Ling-yi Huang and Walter R. L. Lambrecht
Department of Physics, Case Western Reserve University, Cleveland, Ohio 44106-7079, USA
(Received 20 January 2016; revised manuscript received 8 May 2016; published 23 May 2016)

The trends in electronic band structure are studied in the cubic ABX_3 halide perovskites for $A = $ Cs; $B = $ Pb, Sn, Ge, Si; and $X = $ I, Br, Cl. The gaps are found to decrease from Pb to Sn and from Ge to Si, but increase from Sn to Ge. The trend is explained in terms of the atom s levels of the group-IV element and the atomic sizes which changes the amount of hybridization with X-p and hence the valence bandwidth. Along the same series spin-orbit coupling also decreases and this tends to increase the gap because of the smaller splitting of the conduction band minimum. Both effects compensate each other to a certain degree. The trend with halogens is to reduce the gap from Cl to I, i.e., with decreasing electronegativity. The role of the tolerance factor in avoiding octahedron rotations and octahedron edge sharing is discussed. The Ge containing compounds have tolerance factor $t > 1$ and hence do not show the series of octahedral rotation distortions and the existence of edge-sharing octahedral phases known for Pb and Sn-based compounds, but rather a rhombohedral distortion. $CsGeI_3$ is found to have a suitable gap for photovoltaics both in its cubic (high-temperature) and rhombohedral (low-temperature) phases. The structural stability of the materials in the different phases is also discussed. We find the rhombohedral phase to have lower total energy and slightly larger gaps but to present a less significant distortion of the band structure than the edge-sharing octahedral phases, such as the yellow phase in $CsSnI_3$. The corresponding silicon based compounds have not yet been synthesized and therefore our estimates are less certain but indicate a small gap for cubic $CsSiI_3$ and $CsSiBr_3$ of about 0.2 ± 0.2 eV and 0.8 ± 0.6 eV for $CsSiCl_3$. The intrinsic stability of the Si compounds is discussed.

DOI: 10.1103/PhysRevB.93.195211

I. INTRODUCTION

Methylammonium (MA) lead iodide, (MA)PbI_3, and related halide perovskites have recently attracted great attention as solar cell materials [1–8]. In a very short time since their initial development, record photoelectric conversion efficiencies of near 21% have been achieved. Along with the extensive interest this has generated, insights into the fundamental properties of these materials which play a role in the photovoltaic efficiency have emerged. Their strong optical absorption [9], long mean free paths [10] have been addressed. The role of the organic ion and different replacements for methylammonium have been extensively studied. In first approximation it just plays the role of a large positive ion and could potentially be replaced by Cs. However, the symmetry breaking provided by the organic ion dipole also plays a role in the band structure and possibly in the efficiency of the solar cells by reducing the recombination rate [11–14]. The optimum orientation and related vibrational modes of the methylammonium ion in the perovskites has been studied in several papers [15–17]. At high temperature, one may expect the organic ion to be randomly distributed in different orientations and therefore consistent with the overall cubic symmetry. In this paper we instead focus on the purely inorganic compounds with Cs as a positive ion.

From an environmental perspective, Pb is undesirable because of its toxicity. It is thus natural to look for alternative chemical elements to replace it. Sn is a natural choice and hybrid metal-organic Sn halides were studied by Noel *et al.* [18], while inorganic $CsSnI_3$ was studied by Chung *et al.* [19,20]. Ge-based halide compounds both organic and inorganic were considered by Stoumpos *et al.* [21] but mostly from the point of view of nonlinear optics. The band structures of the $CsGeX_3$ compounds have been studied previously by a tight-binding method [22] and the pseudopotential plane-wave method [23] but did not provide accurate gaps in comparison with experiment. Solar cells based on $CsGeI_3$ were very recently realized by Krishnamoorthy *et al.* [24]. Furthermore one may wonder if possibly other substitutions may further improve the properties of these materials. This exploration should be based on a fundamental understanding of the role each element plays in these compounds. In this paper, we present first-principles calculations which may guide this search. In this Introduction, we provide preliminary considerations guiding our choice of materials to study.

Since Pb and Sn in these materials are divalent, a natural choice to replace them would be to consider other divalent elements. With the halogens surrounding them in corner-sharing octahedra, the PbX_3 or SnX_3 units can be thought of as large single negative ions, compensated by $(MA)^+$ or Cs^+ ions. However, this does not mean one may substitute any other divalent ion. In fact, the suitability of these halides for photovoltaics depends strongly on their band structure. In the following subsections, we explain why instead we focus on Ge and Si as replacements for Pb and Sn.

A. Crucial band structure features

In a previous study [9] of $CsSnX_3$ we emphasized that these materials have some unique features in their band structure, which we called "orbital inverted." Their valence band maximum (VBM) consists of antibonding states between the Sn (or Pb) s orbitals and the halogen p orbitals. At the corner of the cubic Brillouin zone of the cubic perovskite, labeled R, the X-p orbitals on opposite faces of the cube have opposite sign, so that the p orbitals all point their same sign lobe towards the center of the cube and hence by symmetry they can interact with the s orbital of Sn or Pb. This then

leads to a nondegenerate strongly dispersing valence band maximum, with a strong Sn (Pb)-s character. The conduction band minimum (CBM) occurs at this same $\mathbf{k}$ point and consists entirely of Sn (Pb)-p states and is threefold degenerate if we do not include spin-orbit coupling. In fact, by symmetry analysis (given in Ref. [9]), the Sn (Pb)-p states cannot interact with the halogen states at the R point of the Brillouin zone, while at other $\mathbf{k}$ points, for example the Γ point, they can and this is why the CBM occurs at R. This is opposite to what occurs in most direct gap tetrahedral semiconductors (such as GaAs), which have a threefold degenerate anion-p-like VBM and a nondegenerate cation-s-like conduction band. Hence the name orbital inverted.

Several points are important here. First, because of the strong components of, respectively, s- and p-like orbitals on the same atom of the VBM and CBM at the same $\mathbf{k}$ point, a strong dipole allowed transition is expected and explains the strong absorption, an obviously important property for a solar cell material. Secondly, the gap is much smaller than expected for such a strongly ionic material. This is because of its largely intra-atomic Sn or Pb character. This strong Sn (Pb)-s to halogen-p interaction in turn comes about because of the relatively deep energy position of the Sn or Pb s states. Their atomic s levels calculated within the local density approximation (LDA) are at $E_s(\mathrm{Sn}) = -10.896$ eV, $E_s(\mathrm{Pb}) = -12.401$ eV, respectively, deeper than the I-p level, which is at $E_p(\mathrm{I}) = -7.327$ eV. These were calculated for free atoms. Typical group IIa (Be, Mg, Ca, Sr, Ba) or IIb (Zn, Cd, Hg) elements have much higher lying s states, well above the halogen-p states, which would lead to a totally different band structure.

The strongly Sn (Pb)-s to X-p hybridization also is responsible for the strong band dispersion near the VBM and hence its small hole mass, which in turn implies good transport properties for holes. In fact, the first use of $CsSnI_3$ in dye sensitized solar cells was based on its role as hole transporter [19]. For the conduction band, the effective masses are somewhat larger and anisotropic. However, the strong spin-orbit coupling in Pb helps to split off a band with strong and more isotropic dispersion. Thus in the Pb case, both electrons and holes have small masses and high mobilities, as reflected in the long effective mean free paths [10]. Of course, the latter also depend on other factors, such as recombination and scattering lifetimes.

The free atom s levels (in LDA) [25] $E_s(\mathrm{Si}) = -10.967$ eV and $E_s(\mathrm{Ge}) = -12.031$ eV are similar to those of Sn and Pb. Thus a qualitatively similar band structure may be expected. However, the tendency to behave as a divalent (as opposed to tetravalent) ion in forming halides decreases from Pb to Sn to Ge to Si. The increased tendency of Sn and Pb for being divalent is related to its shallower p states. They are thus more likely to only use the p electrons in bonding and hang on to the valence s electrons as a lone pair. This may cast some doubt on the stability of the Ge- or Si-based compounds. It turns out that the Ge-based compounds have already been synthesized long ago [26], while the Si-based compounds have not, to the best of our knowledge. We therefore place here more emphasis on the Ge compounds.

The trend with the halogen has already been studied in our previous work. The more electronegative the halogen (Cl > Br > I) the larger the band gaps. So, this reflects the halogen-p character in the VBM. The more electronegative, the deeper these levels and hence the higher the gap. The atomic p levels (in LDA) of I, Br, and Cl are, respectively, $E_p(\mathrm{I}) = -7.327$ eV, $E_p(\mathrm{Br}) = -8.090$ eV, and $E_p(\mathrm{Cl}) = -8.788$ eV. This trend is somewhat compensated by the fact that the lighter elements, which have the higher electronegativity, are also smaller and hence show shorter B-X bonds. Hence the stronger covalent hybridization will increase the valence band width and reduce the gap. This in part explains why the gap changes with halogen are rather moderate in this family of materials.

B. Tolerance factor analysis

A crucial feature for these materials for practical purposes, is their stability with respect to other crystal structures. This is strongly determined by the size of the ions and in perovskites is usually discussed in terms of a tolerance factor $t = R_{AX}/\sqrt{2}R_{BX}$, where R_{AX} and R_{BX} are typical bond distances between the A or B atom with the halogen X. One could view these as a sum of the corresponding ionic radii. If $t < 1$ it indicates that the space between the corner-sharing BX_6 octahedra is too large for the A atom. The response of the system is then to first tilt the octahedra leading to a tetragonal and eventually an orthorhombic phase if tilts are present about two orthogonal axes. These phase transitions have been observed [20] in, for example, $CsSnI_3$ and each step leads to a denser material. The relation of these rotations to soft phonons was studied in Ref. [27]. These rotations of the octahedra lead to slight increases in gap because the orbitals can interact more effectively. This may be beneficial in some cases to get closer to the optimum gap as determined by the Schockley-Queisser limit [28].

However, these systems can also rebond by sharing edges among the octahedra. This leads to structures closer resembling the SnI_2 or PbI_2 layered structures. This can either lead to the formation of the so-called yellow phase in $CsSnI_3$ or a monoclinic phase in $CsSnCl_3$ or eventually to decomposition back into PbI_2 plus (MA)I in (MA)PbI_3. These structures have much higher band gaps and much flatter band-edge states thus making them unsuitable as photovoltaic absorption and transport materials. An important point is that the yellow phase is even denser than the black γ phase, so a $t < 1$ not only indicates octahedral rotations are expected but also these alternative edge-sharing octahedral structures.

From the above it appears that the key to avoid these edge-sharing octahedral structures is to reduce the size of the octahedral building blocks. This could be done by reducing the halogen size (but this will increase the gap, as we will show below) or by reducing the B cation size. This provides our main motivation to investigate Ge and Si as alternatives to Sn and Pb. Table I gives the tolerance factors based on Shannon ionic radii [29] and indicates that the Ge and Si compounds have tolerance factors $t > 1$. This would indicate an increased stability of the cubic perovskite structure. The Ge compounds are known to have a different structural relaxation mechanism to a rhombohedral structure [21,26], but, significantly, do not exhibit the edge-sharing octahedral phases, such as the yellow phase. This indicates that $t > 1$ may indeed be crucial to avoid the edge-sharing octahedral yellow phase. We will show that

TABLE I. Shannon ionic radii (R_i), tolerance factors (t), and calculated (LDA) and experimental lattice constants of cubic perovskites. For Si, no experimental lattice constants are available, so instead we give the GGA optimum lattice constant and place it in parentheses. The experimental values are given with the citation number in brackets.

Ion	R_i (Å)	Compound	t	a_{LDA} (Å)	$a_{\mathrm{expt.\ (GGA)}}$ (Å)
Cs	1.88	$CsSiI_3$	1.110	5.678	(5.892)
Si	0.4	$CsGeI_3$	1.057	5.783	6.05 [26]
Ge	0.53	$CsSnI_3$	0.998	6.088	6.219 [31]
Sn	0.69	$CsPbI_3$	0.970	6.163	6.289 [32]
Pb	0.775	$CsSiBr_3$	1.151	5.298	(5.476)
Cl	1.81	$CsGeBr_3$	1.090	5.407	5.69 [26]
Br	1.96	$CsSnBr_3$	1.025	5.717	5.804 [33]
I	2.2	$CsPbBr_3$	0.993	5.786	5.874 [34]
		$CsSiCl_3$	1.181	5.051	5.283
		$CsGeCl_3$	1.115	5.165	5.47 [26]
		$CsSnCl_3$	1.044	5.482	5.56 [33]
		$CsPbCl_3$	1.009	5.541	5.605 [34]

the rhombohedral phase maintains a band structure close to that of the cubic perovskite phase. Further confirmation of the relation between the tolerance factor and different structural transformations can be found in the case of $RbGeCl_3$. The smaller Rb ion (Shannon radius 1.52 Å) in this case gives $t \approx 1$ and consistently, this material has a similar monoclinic phase to $CsSnCl_3$ [30].

In practice, it has been found that Sn compounds are more difficult to grow in the desired phase than Pb compounds and also that Cs is more difficult than MA. On the other hand, the organic ion presents its own stability problems against reactions with water [11]. It is difficult to judge at this point if these are intrinsic problems or temporary problems still to be overcome by adjusting the growth procedures. Some insight may be gained by calculating their relative energies of formation as we will do in this paper. Based on the above considerations, we here focus on the properties of the series $CsBX_3$, with $B =$ Pb, Sn, Ge, Si and $X =$ I, Br, Cl. The compounds with Pb, Sn, Ge, and Si are, respectively, called trihalogen plumbates, stannates, germanates, and silicates.

II. METHODS

The full-potential linearized muffin-tin orbital (FP-LMTO) method [35,36] is used as a band structure method. This method can either be used with standard density functionals or with the quasiparticle self-consistent (QS) GW method [37]. The latter is a many-body theory perturbation method for the quasiparticle excitations and has the advantage of providing much more reliable band gaps [38]. We use either the LDA [39] or the generalized gradient approximation (GGA) [40] to estimate the lattice constant and as a starting point for the QSGW calculations. The end result of QSGW is independent of which density-functional theory functional we start from but depends on the lattice constant. Where available we use experimental lattice constants. We use a double basis set of smoothed Hankel envelope functions, Cs $spdf$, spd; Ge spd, sp; and I $spdf$, spd, where the two sets correspond to different

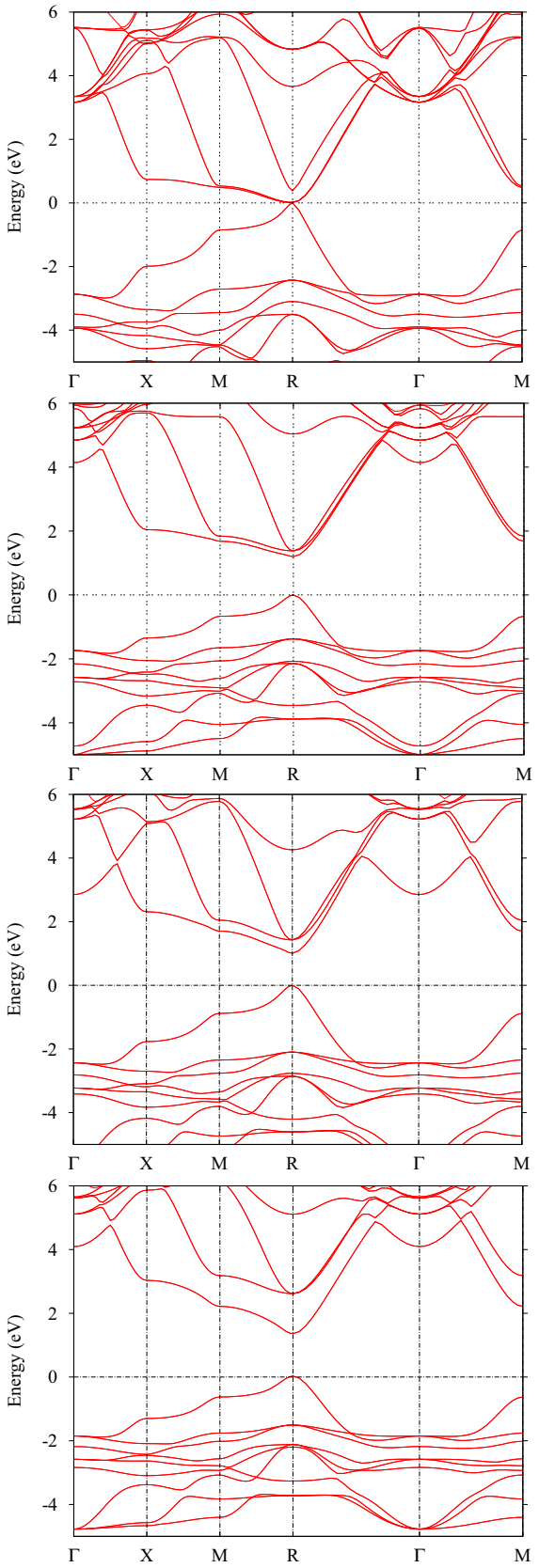

FIG. 1. Band structure, from top to bottom, of cubic $CsSiI_3$, $CsGeI_3$, $CsSnI_3$, and $CsPbI_3$ including spin-orbit interaction and using the QSGW method at the experimental lattice constant, except for the Si case where the calculated LDA lattice constant is used.

smoothing radii and Hankel function energies, and treat I-4*s* states as local orbitals and Cs-5*p* states as band states. For the augmentations inside the spheres in terms of ϕ and $\dot{\phi}$ functions, the angular momentum cutoff is set to $l_{\max} = 4$. A $10 \times 10 \times 10$ k-point mesh is used for the Brillouin zone integrations in the self-consistent calculations. For the GW method, a smaller $5 \times 5 \times 5$ mesh is used, which is found to be sufficient to allow for an accurate interpolation to the finer mesh or for the band structure calculations along symmetry lines. Other convergence factors and parameter choices are similar to those used in Ref. [9].

III. RESULTS

A. Band structures of cubic perovskites

Our results for the lattice constants of the cubic phases are given in Table I along with the experimental values where available. As usual the LDA underestimates the lattice constants. We note that at present no experimental data are available for Si-based compounds, because they have not been synthesized, to the best of our knowledge. Therefore we calculate both the LDA and GGA lattice constants which are likely to provide a lower and upper limit, respectively. The band structure calculations at both lattice constants then correspondingly will provide an estimate of the uncertainty on their band gaps.

In Fig. 1 we show the QSGW band structures of cubic $CsBI_3$ with B = Pb, Sn, Ge, and Si. These band structures include spin-orbit coupling and were calculated at the experimental lattice constant, where available; that is, for all except the Si case, where we used the LDA calculated lattice constant. The basic orbital character of the bands was already discussed in the Introduction and for further information we refer the reader to Ref. [9]. One can see a similar overall band structure in all cases. The gaps decrease from Pb to Sn and from Ge to Si. However, it increases from Sn to Ge. The decreasing trend results from the trend in the size of the atoms and hence bond lengths: the shorter the bond length the stronger the hybridization and hence the larger the valence bandwidth and the smaller the band gap. However, the position of the B-s level also plays a role. The closer it is to the X-p the stronger the hybridization. Thus the increase in gap from Sn to Ge results from the deeper Ge-s level, which shifts the whole VB down.

The second trend we observe in Fig. 1 is a decreasing spin-orbit splitting of the CBM. This is expected as the spin-orbit splitting is decreasing for lighter (lower Z) elements. In fact, if we had neglected spin-orbit coupling the gaps of $CsPbI_3$ and $CsSnI_3$ would be 2.288 and 1.354 eV, respectively. It is because of the much stronger spin-orbit coupling in Pb that the gap is reduced to 1.331 eV when spin-orbit coupling is included. On the other hand, the gap increase from Sn to Ge results in part also from the much smaller spin-orbit coupling in Ge compared to Sn.

The band gaps are summarized in Table II. When we evaluate the gap at the LDA lattice constant, which is underestimated, the gap is smaller than the one with the experimental lattice constant. In fact, for the Pb, Sn, and Ge case, using the LDA lattice constant would have given a significant underestimate of the gap by 30%, 55%, and 61% even though the lattice constants were only underestimated by 2%, 2.1%, and 4.4%. These gap changes with lattice constant appear anomalously large. This illustrates another

TABLE II. Band gaps and band-gap deformation potentials (in eV) of various halide perovskites in different methods. The values were calculated at the experimental lattice constants except for Si compounds, where we give the results both at LDA and GGA lattice constants. For the other cases, gaps at the LDA calculated lattice constant are given in parentheses. The experimental values are given with the citation number in brackets.

Compound	LDA (GGA)	QSGW	QSGW+SO	Expt.	$dE_g/d\ln V$
α-$CsSiI_3$	−0.604[a]	−0.328	0.020		6.4
	−0.143[b]	0.380	0.313		
α-$CsGeI_3$	0.746	1.404	1.199 (0.465 [a])		5.4
α-$CsSnI_3$	0.295	1.354	1.008 (0.452[a])		8.7
α-$CsPbI_3$	1.261	2.288	1.331 (0.940[a])		6.4
α-$CsSiBr_3$	−0.871[a]	−0.433	0.029		7.5
	−0.314[b]	0.412	0.381		
α-$CsGeBr_3$	0.867	1.948	1.800 (0.710[a])		7.1
α-$CsSnBr_3$	0.351	1.690	1.382 (0.985[a])		8.7
α-$CsPbBr_3$	1.384	2.784	1.868 (1.529[a])		7.5
α-$CsSiCl_3$	−0.649[a]	0.161	0.137		9.5
	0.226[b]	1.450	1.427		
α-$CsGeCl_3$	1.302	2.791	2.654 (1.461[a])		6.9
α-$CsSnCl_3$	0.744	2.997	2.693 (2.313[a])	2.9 [41]	9.0
α-$CsPbCl_3$	1.782	3.589	2.678 (2.411[a])		7.7
β-$CsSnI_3$	0.453	1.494	1.288		
β-$CsSnBr_3$	0.574	1.918	1.740	1.8 [42]	
α-(MA)PbI_3	1.276	2.557	1.675	1.61 [43]	
γ-$CsSnI_3$	0.503	1.5	1.3	1.3 [44,45]	

[a]At LDA lattice constant.
[b]At GGA lattice constant.

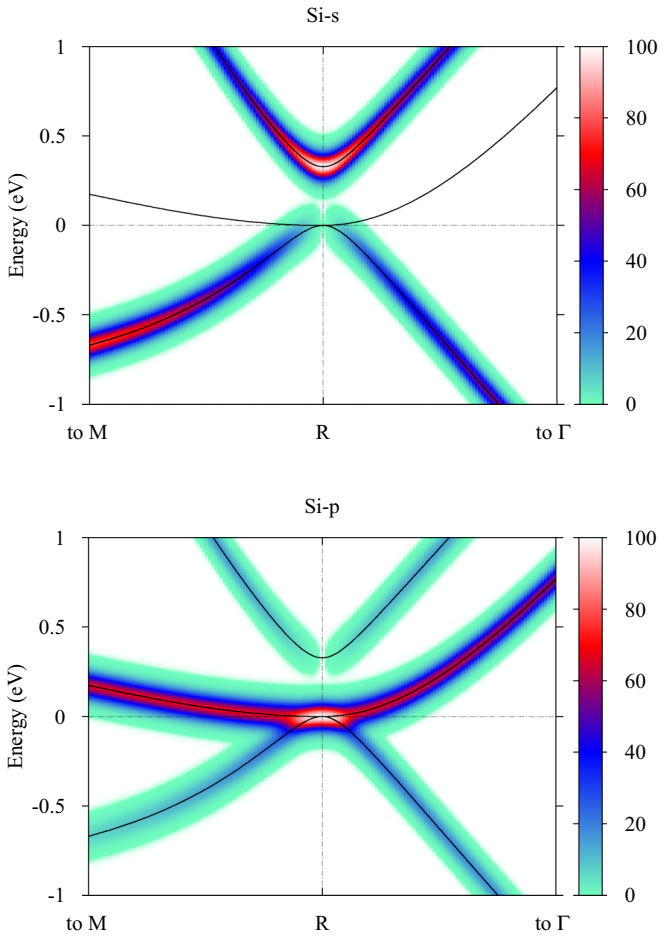

FIG. 2. Bands without spin-orbit coupling near the gap at R projected on Si-s and Si-p states. The lower triply degenerate band at R is R_{15}; the upper nondegenerate one is R_1.

anomalous point about these materials: the gap decreases with decreasing lattice constant because it arises from the change in valence bandwidth. The band gap deformation potentials $dE_g/d\ln V$ are included in Table II and are typical values for semiconductors. The main reason for the gap underestimate is that the LDA lattice constants are more than usually underestimated.

For $CsSiI_3$, the gap actually closes if we use the LDA lattice constant, and is quite small, 0.380 eV, if we use the GGA lattice constant. The gap closing is interesting because the Fermi level becomes pinned at the R_{15} degenerate level, which in the other compounds is the CBM. The R_1 level, which in the other compounds is the VBM, now lies above it, so the gap becomes in some sense negative or inverted. One can furthermore see the inversion by coloring the bands according to their Si-s and Si-p characters (see Fig. 2). One can clearly see that the lowest band starts out s-like toward M (or Γ), loses its s-like character and becomes p-like right near R. The upper band instead is s-like near R but loses its s character away towards the M point. The p character is concentrated in the middle band but the upper and lower bands also have a bit of p character away from the R point. The gaps in Table II for the Si compounds indicate the $R_{15} - R_1$ gap, (which is thus negative) except when spin-orbit coupling is included. Including spin-orbit coupling, a small gap of 20 meV opens because of the splitting of the R_{15} state as shown in Fig. 3. This situation indicates a topological insulator character of the band structure.

We can also see that the CBM moves away from R. This is another manifestation of the spin-orbit coupling. Because there is no electric field or symmetry breaking from the cubic structure, this can be identified with the Dresselhaus effect [46]. Note that it is much smaller than the similar splitting of the CBM one sees in $(MA)PbI_3$ with ordered MA molecules and hence dipoles that break the cubic symmetry and add an electric field and hence lead to the Bychkov-Rashba effect [47,48].

For the Br case, the band-gap situation is also inverted, while for Cl already a small gap opens in QSGW even when using the LDA lattice constant. This would be rather interesting but still rather uncertain because of the uncertainty in lattice constant. When we use the larger GGA lattice constants, which are in fact, probably closer to experiment, a small gap opens in QSGW for all cases and the band gap is no longer topological. For $CsSiCl_3$ the gap in fact becomes fairly large. As a conservative estimate one might take the average between the results at the LDA and the GGA lattice constants, although this is likely an underestimate of the gap as the GGA lattice constant is expected to be closer to the experimental gap from the corresponding results for the Ge, Sn, and Pb compounds. This leads to a gap of 0.2 ± 0.2 eV

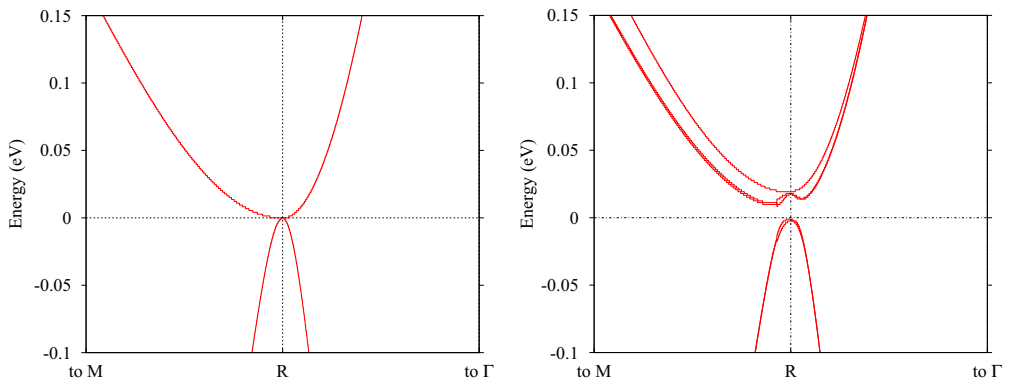

FIG. 3. An even closer view of the band edge of $CsSiI_3$ without (left) and with (right) spin-orbit coupling.

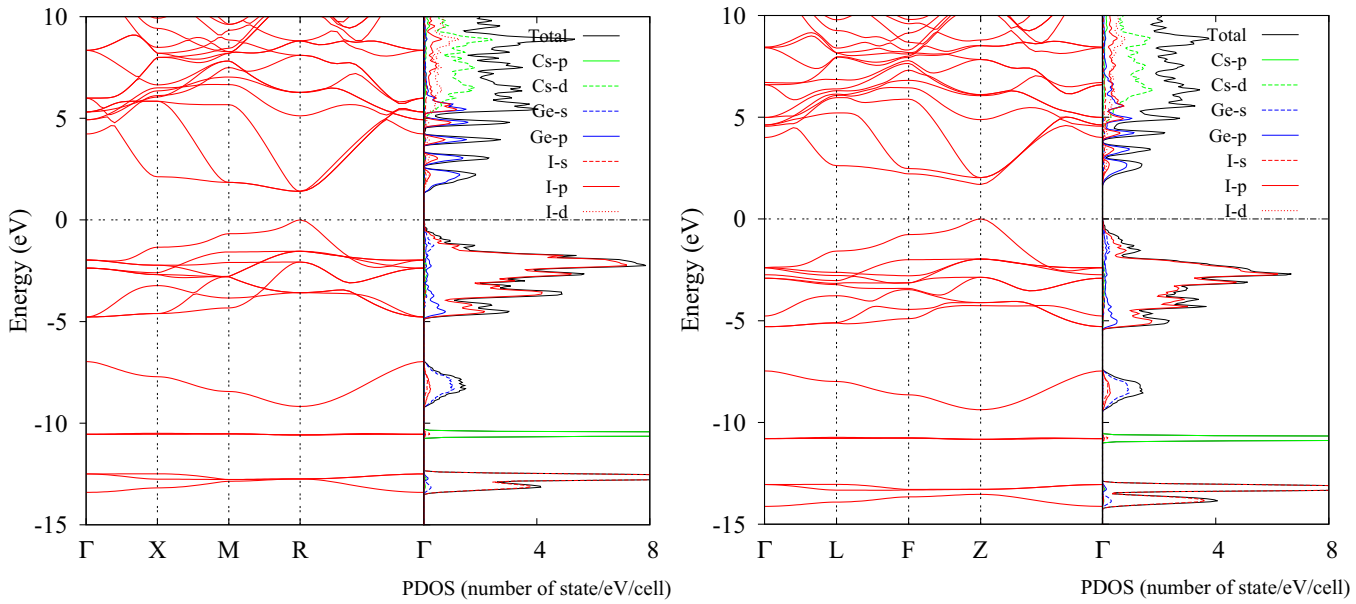

FIG. 4. QSGW band structure without SO of the cubic $CsGeI_3$ (left) and the rhombohedral $CsGeI_3$ (right). In the Brillouin zone of the rhombohedral phase, we follow the notation by Setyawan and Curtarolo [51].

for the I and Br case and 0.8 ± 0.6 eV for the Cl case. This means that the $CsSiCl_3$ gap could in fact be within the range of interest for photovoltaic applications. The uncertainty on the lattice constants resulting from the different density functionals leads to rather large uncertainty on the gaps. The results also indicate that under pressure $CsSiI_3$ and $CsSiBr_3$ may become topological insulators. This has been suggested before by Yang *et al.* [49] for various halides and more recently by Liu *et al.* for $CsPbI_3$ [50]. However, both of these relied on LDA or GGA calculations which underestimate the gaps and thus more easily lead to band inversion.

We should keep in mind that these are for the cubic structure. For the orthorhombic γ structure of $CsSnI_3$ the gap increases to 1.3 eV and is closer to the ideal value for single junction solar cells. For $CsGeI_3$, the gap of 1.199 eV is close to optimal for solar cells and we may expect that the distorted $CsGeI_3$ has a larger gap. Therefore we next study the differences in band structure between the cubic and rhombohedral phases.

B. Band structures of rhombohedral structure

For $CsGeX_3$, the cubic phase exists at high temperatures. Lowering temperatures makes $CsGeX_3$ undergo a phase transition from the cubic phase to the rhombohedral phase [26]. We show our QSGW band structure for the cubic (α) and the rhombohedral $CsGeI_3$ in Fig. 4. The first thing to notice is that the overall band structure is very similar in both structures. Thus the rhombohedral distortion does not disrupt the key features of the band structure which we mentioned in the Introduction. The difference is mainly that the threefold degenerate CBM splits in the rhombohedral phase because of the crystal field splitting or symmetry lowering. In this figure, we also indicate the partial densities of states. These confirm that in both structures, the conduction band minimum consists primarily of Ge-p states. The upper valence band consists mainly of I-p states but near the top we can recognize a sizable Ge-s component. These are antibonding combinations of I-p and Ge-s. The corresponding bonding states, here form a separate band centered near -7 eV. The very flat band below -10 eV is due to the Cs-5p semicore states, while the lower band corresponds to the I-s states.

We summarize the gaps of rhombohedral $CsGeX_3$ in Table III. The gap of the rhombohedral $CsGeI_3$ is about 1.6 eV, which is still quite good for single junction solar cell applications. The $CsGeBr_3$ and $CsGeCl_3$ compounds on the other hand, have significantly larger gaps already in the α phase, and even larger in the rhombohedral phase. These are unsuitable for photovoltaics, but may still find other interesting properties, such as nonlinear optical properties [21].

TABLE III. Band gaps (in eV) of rhombohedral $CsGeX_3$ in different methods.

Compound	LDA	QSGW	QSGW+SO	Other calculations	Experimental data
$CsGeI_3$	0.804	1.690	1.619	1.25[a]	1.6[b], 1.51[a]
$CsGeBr_3$	1.088	2.695	2.654	4.74[c], 2.37[a]	2.32[c], 2.38[a]
$CsGeCl_3$	1.973	4.374	4.309	7.91[c], 2.59[a]	3.67[c], 3.43[a]

[a]L. Kang *et al.* [52], calculated by the screened exchange LDA method.
[b]C. C. Stoumpos *et al.* [21].
[c]D.-K. Seo *et al.* [22], calculated by the extended Hückel tight-binding method.

C. Structural stability

We next discuss the structural stability aspects. The rhombohedral phases are found to be lower in energy than the cubic phase by 0.147 eV/f.u. in $CsGeI_3$, 0.163 eV in $CsGeBr_3$, and 0.172 eV in $CsGeCl_3$. These energy differences are similar to the γ-α energy difference in $CsSnI_3$. For comparison, $CsSnI_3$ is found to be unstable in the cubic form vs CsI and SnI_2 by 0.038 eV. In other words, the cubic phase has positive energy of formation. In addition it is unstable in the sense of having soft phonons [27]. The latter are avoided in the γ phase by suitably rotating the octahedrons and the γ phase is then found to have a negative energy of formation by -0.103 eV. Importantly, for $CsSnI_3$ we found the yellow phase to have a lower energy by 0.19 eV per formula unit than the γ phase. This result differs from da Silva *et al.* [53] who found the γ and yellow phases to have almost identical energies of formation. Calculating relative energies of such rather differently bonded structures requires great precision and thus these results may require further scrutiny. But either way, they indicate that the two structures are close in energy and this may explain why experimentally, in $CsSnI_3$, avoiding the competing yellow phase is a significant problem. As documented by Chung *et al.* [20], which phase occurs depends on the growth method. The yellow phase occurs first when growing from solution, while the black phase only occurs when starting from a melt or after heating of the yellow phase. Second, the yellow phase reappears from the γ phase after prolonged exposure to air.

Significantly, for $CsGeI_3$ there is no competing "yellow" phase known. As we discussed earlier, the latter is not expected because the tolerance factor $t > 1$ so there is no need for compression of the structure. The rhombohedral structure is in fact the stable structure at low temperatures. It results from the fact that compared to Sn and Pb, Ge has a stronger tendency to form sp^3 hybrids and let both s and p electrons participate in the bonding. By letting the Ge move off center along the diagonal in its octahedral surroundings, it allows a stronger bonding to three of its halogen neighbors than the other three. In other words, it prefers to make fewer but stronger bonds.

Finally, we consider the intrinsic stability of $CsSiI_3$. If SiI_2 would exist in the same structure as SnI_2, that energy of reaction is -0.350 eV. However, SiI_2 exists in the form Si_5I_{10} [54]. Using this crystal structure as reference, we find a positive energy of formation of 0.140 eV. We also examine the reaction

$$CsI + SiI_4 \rightarrow CsSiI_3 + I_2(\text{solid}), \qquad (1)$$

which gives also a positive energy of 0.941 eV. Clearly what we are battling here is that Si strongly prefers to be in a tetravalent state, SiI_4, rather than divalent in SiI_2. This indicates that it is unlikely that $CsSiI_3$ could be synthesized using equilibrium growth techniques. Nonetheless we cannot exclude that nonequilibrium growth may succeed in forming this material. Also, we have not yet investigated the possibility that $CsSiI_3$ could be stabilized by a similar rhombohedral transformation as $CsGeI_3$. Finally, the more reactive Br and Cl lead to the existence of $SiBr_2$ and $SiCl_2$ molecules or radicals which could make the possible synthesis of $CsSiBr_2$ and or $CsSiCl_3$ somewhat more likely. These questions need further investigation.

IV. CONCLUSIONS

In summary, we have discussed here several rationales to study halide perovskites including Ge and possibly Si beyond the more fully explored Sn and Pb. First, they are a natural extension of this family of materials, which still preserves the same basic band structures. Secondly, the smaller lattice constants may prevent the tendency of these materials toward edge sharing of octahedra even with smaller A ions such as Cs instead of methylammonium. This in turn could avoid some of the chemical stability problems of the organic ion component in aqueous environments. We found that rhombohedral $CsGeI_3$ as well as cubic $CsGeI_3$ both have suitable band gaps for solar cells. The Si compounds were here only studied in the cubic α phase and were found to have significantly smaller gaps, except for $CsSiCl_3$, for which we found a gap of 1.4 eV at the GGA lattice constant. Rhombohedral distortions may also be expected for the silicates, similar to the germanates because of their tolerance factor $t > 1$ and could slightly increase the gap. These gaps are also more uncertain because of the uncertainty in the lattice constant. While unfortunately $CsSiI_3$ was found to be intrinsically unstable, the bromide and chloride may be slightly more promising. Their possible synthesis remains an open question.

ACKNOWLEDGMENTS

This work was supported by the U.S. Department of Energy, Office of Science, Basic Energy Sciences under Grant No. DE-SC0008933. Calculations made use of the High Performance Computing Resource in the Core Facility for Advanced Research Computing at Case Western Reserve University.

[1] A. Kojima, K. Teshima, Y. Shirai, and T. Miyasaka, J. Am. Chem. Soc. **131**, 6050 (2009).
[2] M. M. Lee, J. Teuscher, T. Miyasaka, T. N. Murakami, and H. J. Snaith, Science **338**, 643 (2012).
[3] J. M. Ball, M. M. Lee, A. Hey, and H. J. Snaith, Energy Environ. Sci. **6**, 1739 (2013).
[4] G. E. Eperon, V. M. Burlakov, P. Docampo, A. Goriely, and H. J. Snaith, Adv. Funct. Mater. **24**, 151 (2014).
[5] M. Liu, M. B. Johnston, and H. J. Snaith, Nature (London) **501**, 395 (2013).
[6] J. Burschka, N. Pellet, S.-J. Moon, R. Humphry-Baker, P. Gao, M. K. Nazeeruddin, and M. Grätzel, Nature (London) **499**, 316 (2013).
[7] H.-S. Kim, S. H. Im, and N.-G. Park, J. Phys. Chem. C **118**, 5615 (2014).
[8] N.-G. Park, Mater. Today **18**, 65 (2015).

[9] L.-y. Huang and W. R. L. Lambrecht, Phys. Rev. B **88**, 165203 (2013).

[10] S. D. Stranks, G. E. Eperon, G. Grancini, C. Menelaou, M. J. P. Alcocer, T. Leijtens, L. M. Herz, A. Petrozza, and H. J. Snaith, Science **342**, 341 (2013).

[11] J. M. Frost, K. T. Butler, F. Brivio, C. H. Hendon, M. van Schilfgaarde, and A. Walsh, Nano Lett. **14**, 2584 (2014).

[12] M. R. Filip, G. E. Eperon, H. J. Snaith, and F. Giustino, Nat. Commun. **5**, 5757 (2014).

[13] C. Quarti, E. Mosconi, and F. D. Angelis, Chem. Mater. **26**, 6557 (2014).

[14] F. Zheng, L. Z. Tan, S. Liu, and A. M. Rappe, Nano Lett. **15**, 7794 (2015).

[15] T. Glaser, C. Müller, M. Sendner, C. Krekeler, O. E. Semonin, T. D. Hull, O. Yaffe, J. S. Owen, W. Kowalsky, A. Pucci *et al.*, J. Phys. Chem. Lett. **6**, 2913 (2015).

[16] A. M. A. Leguy, J. M. Frost, A. P. McMahon, V. G. Sakai, W. Kockelmann, C. Law, X. Li, F. Foglia, A. Walsh, B. C. O'Regan *et al.*, Nat. Commun. **6**, 7124 (2015).

[17] J. Ma and L.-W. Wang, Nano Lett. **15**, 248 (2015).

[18] N. K. Noel, S. D. Stranks, A. Abate, C. Wehrenfennig, S. Guarnera, A.-A. Haghighirad, A. Sadhanala, G. E. Eperon, S. K. Pathak, M. B. Johnston *et al.*, Energy Environ. Sci. **7**, 3061 (2014).

[19] I. Chung, B. Lee, J. He, R. P. H. Chang, and M. G. Kanatzidis, Nature (London) **485**, 486 (2012).

[20] I. Chung, J.-H. Song, J. Im, J. Androulakis, C. D. Malliakas, H. Li, A. J. Freeman, J. T. Kenney, and M. G. Kanatzidis, J. Am. Chem. Soc. **134**, 8579 (2012).

[21] C. C. Stoumpos, L. Frazer, D. J. Clark, Y. S. Kim, S. H. Rhim, A. J. Freeman, J. B. Ketterson, J. I. Jang, and M. G. Kanatzidis, J. Am. Chem. Soc. **137**, 6804 (2015).

[22] D.-K. Seo, N. Gupta, M.-H. Whangbo, H. Hillebrecht, and G. Thiele, Inorg. Chem. **37**, 407 (1998).

[23] L.-C. Tang, C.-S. Chang, L.-C. Tang, and J. Y. Huang, J. Phys.: Condens. Matter **12**, 9129 (2000).

[24] T. Krishnamoorthy, H. Ding, C. Yan, W. L. Leong, T. Baikie, Z. Zhang, M. Sherburne, S. Li, M. Asta, N. Mathews *et al.*, J. Mater. Chem. A **3**, 23829 (2015).

[25] Although the Hartree-Fock atomic levels (taken from [55]) follow a somewhat different sequence, $E_s(\mathrm{Si}) = -14.79$ eV, $E_s(\mathrm{Ge}) = -15.16$ eV, $E_s(\mathrm{Sn}) = -13.04$ eV, $E_s(\mathrm{Pb}) = -12.49$ eV, the important point is that these are all deeper than the halogen-p and close enough to it to have significant hybridization.

[26] G. Thiele, H. W. Rotter, and K. D. Schmidt, Z. Anorg. Allg. Chem. **545**, 148 (1987).

[27] L.-y. Huang and W. R. L. Lambrecht, Phys. Rev. B **90**, 195201 (2014).

[28] W. Shockley and H. J. Queisser, J. Appl. Phys. **32**, 510 (1961).

[29] R. D. Shannon, Acta Crystallogr., Sect. A: Found. Adv. **32**, 751 (1976).

[30] D. Messer, Z. Naturforsch. B **33**, 366 (1978).

[31] K. Yamada, S. Funabiki, H. Horimoto, T. Matsui, T. Okuda, and S. Ichiba, Chem. Lett. **20**, 801 (1991).

[32] D. M. Trots and S. V. Myagkota, J. Phys. Chem. Solids **69**, 2520 (2008).

[33] J. Barrett, S. R. A. Bird, J. D. Donaldson, and J. Silver, J. Chem. Soc. A **1971**, 3105 (1971).

[34] C. K. Møller, Nature(London) **182**, 1436 (1958).

[35] M. Methfessel, M. van Schilfgaarde, and R. A. Casali, in *Electronic Structure and Physical Properties of Solids. The Use of the LMTO Method*, edited by H. Dreyssé, Lecture Notes in Physics Vol. 535 (Springer-Verlag, Berlin, 2000), p. 114.

[36] T. Kotani and M. van Schilfgaarde, Phys. Rev. B **81**, 125117 (2010).

[37] T. Kotani, M. van Schilfgaarde, and S. V. Faleev, Phys. Rev. B **76**, 165106 (2007).

[38] M. van Schilfgaarde, T. Kotani, and S. Faleev, Phys. Rev. Lett. **96**, 226402 (2006).

[39] U. von Barth and L. Hedin, J. Phys. C **5**, 1629 (1972).

[40] J. P. Perdew, K. Burke, and M. Ernzerhof, Phys. Rev. Lett. **77**, 3865 (1996).

[41] A. Voloshinovskii, S. V. Myagkota, N. S. Pidzyrailo, and M. V. Tokarivskii, J. Appl. Spectrosc. **60**, 226 (1994).

[42] S. J. Clark, C. D. Flint, and J. D. Donaldson, J. Phys. Chem. Solids **42**, 133 (1981).

[43] Y. Yamada, T. Nakamura, M. Endo, A. Wakamiya, and Y. Kanemitsu, Appl. Phys. Express **7**, 032302 (2014).

[44] K. Shum, Z. Chen, J. Qureshi, C. Yu, J. J. Wang, W. Pfenninger, N. Vockic, J. Midgley, and J. T. Kenney, Appl. Phys. Lett. **96**, 221903 (2010).

[45] Z. Chen, C. Yu, K. Shum, J. J.Wang, W. Pfenninger, N. Vockic, J. Midgley, and J. T.Kenney, J. Luminescence **132**, 345 (2012).

[46] G. Dresselhaus, Phys. Rev. **100**, 580 (1955).

[47] Y. A. Bychkov and E. I. Rashba, J. Phys. C **17**, 6039 (1984).

[48] E. I. Rashba, Sov. Phys. Solid State **2**, 1109 (1960).

[49] K. Yang, W. Setyawan, S. Wang, M. B. Nardelli, and S. Curtarolo, Nat. Mater. **11**, 614 (2012).

[50] S. Liu, Y. Kim, L. Z. Tan, and A. M. Rappe, Nano Lett. **16**, 1663 (2016).

[51] W. Setyawan and S. Curtarolo, Comput. Mater. Sci. **49**, 299 (2010).

[52] L. Kang, D. M. Ramo, Z. Lin, P. D. Bristowe, J. Qin, and C. Chen, J. Mater. Chem. C **1**, 7363 (2013).

[53] E. L. da Silva, J. M. Skelton, S. C. Parker, and A. Walsh, Phys. Rev. B **91**, 144107 (2015).

[54] Ch. Kratky, H. Hengge, H. Stüger, and A. L. Rheingold, Acta Cryst. **C41**, 824 (1985).

[55] W. A. Harrison, *Elementary Electronic Structure* (World Scientific, Singapore, 1999).